

Modulation of snow on the daily evolution of surface heating over the Tibetan Plateau during winter: Observational analyses

Yufei Xin¹, ge Liu¹, and Yueli Chen¹

¹Chinese Academy of Meteorological Sciences

November 23, 2022

Abstract

Studying the daily evolution of turbulent fluxes modulated by snowfall over the Tibetan Plateau (TP) is of importance to understand the features of the change in the TP heat source/sink. Based on observations from 4 sites of the Third TP Atmospheric Scientific Experiment, the process of surface energy balance impacted by snow is investigated. The results show that the surface albedo increases on the first day of snow and then slowly decreases. Correspondingly, the sensible heat (H) flux sharply decreases after snow and then recovers to the original level during the following approximately 10 days. The latent heat (LE) flux becomes more active and stronger after snowfall and persists for a longer period than H, since the soil moisture may still contribute to a high LE after snowmelt. As the synergistic result of H and LE modulated by snow, the surface turbulent heating (i.e., the sum H and LE) of the TP decreases at the early period of snow events and then even enhances to a higher level after the snowmelt than before snow. Comparison analyses reveal that the impact of snow on the H and LE over the TP is much stronger than over similar latitude low-altitude regions in North America and Europe, which may be partly attributed to the larger and more drastic change of the surface net solar radiation associated with snow processes in the TP. This study may help further understand the detailed physical processes of modulation of snow events on Asian weather processes during winter.

Modulation of snow on the daily evolution of surface heating over the Tibetan Plateau during winter: Observational analyses

Yufei XIN^{1*}, Ge Liu^{1,2*}, Yueli Chen¹

¹*State Key Laboratory of Severe Weather, Chinese Academy of Meteorological Science, Beijing, China*

²*Collaborative Innovation Centre on Forecast and Evaluation of Meteorological Disasters, Nanjing University of Information Science and Technology, Nanjing, China*

Corresponding author:

Drs. Yufei Xin and Ge Liu

State Key Laboratory of Severe Weather, Chinese Academy of Meteorological Sciences, 46 Zhong-Guan-Cun South Avenue, Beijing 100081, China.

Email: xinyf@cma.gov.cn;

liuge@cma.gov.cn

Telephone: 86-10-68407867

1 **Abstract:** Studying the daily evolution of turbulent fluxes modulated by snowfall
2 over the Tibetan Plateau (TP) is of great importance to understand the features of the
3 change in the TP heat source/sink and its contribution to Asian atmospheric
4 circulation and weather processes. However, the lack of data over the TP restricts the
5 detailed studies. Based on observations from 4 sites of the Third TP Atmospheric
6 Scientific Experiment, the process of surface energy balance impacted by snow is
7 investigated. The results show that the surface albedo largely increases on the first day
8 of snow and then slowly decreases. Correspondingly, the sensible heat (H) flux
9 sharply decreases after snow and then gradually recovers to the original level during
10 the following approximately 10 days. The latent heat (LE) flux becomes more active
11 and stronger after snowfall and persists for a longer period than H, since the soil
12 moisture may still contribute to a high LE after snowmelt. As the synergistic result of
13 H and LE modulated by snow, the surface turbulent heating (i.e., the sum H and LE)
14 of the TP decreases at the early period of snow events and then even enhances to a
15 higher level after the snowmelt than before snow. Comparison analyses reveal that the
16 impact of snow on the H and LE over the TP is much stronger than over similar
17 latitude low-altitude regions in North America and Europe, which may be partly
18 attributed to the larger and more drastic change of the surface net solar radiation
19 associated with snow processes in the TP. The ERA5 and CFS reanalysis datasets fail
20 to reproduce the modulation of snow on the heat fluxes, which suggests that the
21 physical schemes of the models should be further improved based on the
22 observational analyses over TP. This study may help further understand the detailed
23 physical processes of modulation of snow events on Asian weather processes during
24 winter and is also conducive to the improvement of surface parameterization schemes
25 of models.

26 **Key words:** Tibetan Plateau snow, eddy-covariance heat flux, ERA5 reanalysis, CFS
27 reanalysis.

28 **1. Introduction**

29 The Tibetan Plateau (TP), located at the subtropical central and eastern Eurasian

30 continent, is the highest in the world, with a mean elevation higher than 4000 m above
31 sea level. The TP generally acts as an elevated atmospheric heat source during
32 summer but a heat sink during winter (Flohn, 1957; Yeh et al. 1957). The heat
33 source/sink plays an important part in modulating weather and climate over the TP
34 adjacent and even broader regions. The elevated heat source of the TP should be
35 considered as one of the most important factors that drive the South and East Asian
36 summer monsoons (Yin et al., 1949; Flohn, 1957; Yeh et al. 1957). Based on different
37 datasets and numerical experiments, the contribution of the TP thermal anomaly to the
38 seasonal transition of atmospheric circulation and the associated onset of the Asian
39 monsoon has been revealed by many studies (Yeh and Gao 1979; Shen et al. 1984;
40 Nitta, 1983; Luo and Yanai, 1983, 1984; Tao and Chen, 1987; He et al. 1987; Yanai
41 et al. 1992, 2006; Yanai and Li, 1994; Wu et al. 1997, 2003, 2004; Liu et al. 2001,
42 2002; Duan and Wu 2005). Recent studies have argued that the thermal anomaly of
43 the TP may adjust the atmospheric circulation and associated climate variability over
44 East Asia, the Pacific, Europe, and even Africa (Duan et al., 2013; Duan and Wu,
45 2005; Liu et al., 2017, 2015; Wu et al., 2016; Lu et al., 2018; Chen et al., 2020; Nan et
46 al., 2019, 2020), showing a broader effect during summer.

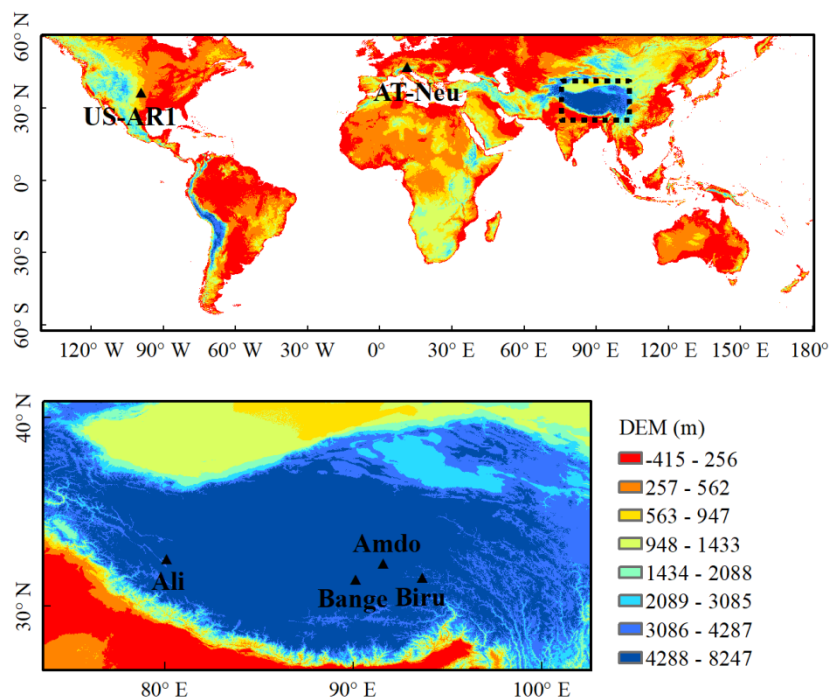
47 In earlier research, the TP was regarded as a large-scale topography that blocks and
48 modulates the atmospheric circulation (Queney 1948, Charney and Eliassen 1949,
49 Bolin 1950, Yeh 1950). Such an effect of dynamical blocking is more crucial in
50 winter (Ma et al. 2014). Besides, many studies that reported the cross-season
51 relationship between the winter snow cover anomaly in the TP and summer monsoon

52 and associated rainfall anomalies over India (Dey and Bhanukumar 1983; Dey et al.
53 1985; Dey and Kathuria 1986), and East Asia (Tao and Chen, 1987; Xu et al. 1994;
54 Wei and Luo, 1994; Zhai and Zhou, 1997; Wu and Qian, 2000; Chen et al. 2000; Wu
55 et al. 2003). However, fewer studies focus on the winter snow and the related heating
56 effect of the TP on the simultaneous weather and climate variability. Nan et al. (2012)
57 revealed that the atmospheric cold source around the TP can result in atmospheric
58 circulation and associated precipitation anomalies over central-eastern China during
59 January. Li et al. (2018) found that through modulating the sensible (H) and latent
60 (LE) heat fluxes, the TP snow cover has a significant influence on the Asian
61 atmospheric circulation and weather on medium-range time scales during winter.

62 Obviously, investigating the short-time (e.g., daily) evolution of the H and LE
63 modulated by the TP snowfall is of great benefit to further understand the effect of the
64 heat source/sink of the TP and its potential contribution to Asian atmospheric
65 circulation and weather processes. However, the lack of data over the TP restricts
66 detailed studies. In recent years, through the Third Tibetan Plateau Atmospheric
67 Scientific Experiment (TIPEX-III; Zhao et al., 2016b, Xin et al. 2018), updated
68 observational eddy-covariance and planetary boundary layer data have been obtained.
69 The observational data provide a possibility to further study this snowfall-related
70 daily evolution of H and LE.

71 This rest of the paper is organized as follows. The data are described in Section 2.
72 The results are presented in Section 3. Finally, a summary and related discussions are
73 provided in Section 4.

74 **2. Study Area and Data**



75

76 **Figure 1** The locations of the observation sites, including US-AR1 and CA-NS7 in North America,
77 AT-Neu in Europe, Ali (AL), Bange (BG), Amdo (AD), and Biru (BR) in the TP. The TP domain is
78 shown in the bottom amplifactory figure. The color shadings denote the altitude of topography.

79 The geographic information and land surface characteristics of the observation
80 sites are shown in Table 1. Figure 1 presents the locations of these sites, including
81 four sites in the TP and two low-altitude grassland sites in Europe and North America,
82 respectively. The observational data from four sites at the TP were obtained from the
83 TIPEX-III (Zhao et al. 2016) that started in the summer of 2014 and continues to be
84 conducted. There are ten sites that are involved in the land-atmospheric interaction
85 mission of TIPEX-III (Xin et al. 2018). However, only the data from the four sites
86 were used in this study since most of the winter observational data from the other six
87 sites are missing or fail to pass the quality control test. The shortwave (SW) radiation,
88 longwave (LW) radiation, air temperature, amount of precipitation, and the other

89 variables at a temporal resolution of 30 min were obtained from the slow-response
90 sensor for the atmospheric gradient and solar radiation. The turbulent fluxes, which
91 were obtained from fast-response sensors for sonic anemometers and gas analyzers,
92 have been processed by flux correction from raw eddy-covariance data (Xin et al.,
93 2018). The data for the two sites in low-altitude Europe and North America (Figure 1)
94 were acquired from the FLUXNET dataset (<https://fluxnet.fluxdata.org/>). Similar to
95 the four sites in the TP, the two low-altitude sites are also covered by grassland or
96 bare soil and possess snow cover in winter. Moreover, the latitudes of the two sites are
97 as close to the TP sites as possible. The Woodward Switchgrass 1 site (US-AR1),
98 obtained from the U.S. Department of Agriculture Southern Plains Range Research
99 Station in Woodward, Oklahoma, has 4 years of data, beginning at 0:00 on January 1
100 2009 (2002) and ending at 23:30 on December 31, 2012 (2005). The Neustift site
101 (AT-Neu), owned by the University of Innsbruck, has 7 years of data from 0:00 on
102 January 1, 2006, to 23:30 on December 31, 2012. Additionally, the National Centers
103 for Environmental Prediction (CFS) 4-time daily reanalysis dataset (Kanamitsu et al.,
104 2002) and the ERA5 24-time daily reanalysis dataset (Sabater et al., 2019) from
105 European Centre for Medium-Range Weather Forecasts (ECMWF) were used in this
106 study.

107 **Table 1.** Information of observational sites in this study

| <i>Site</i> | <i>Geographical information</i> | | | <i>Land cover type</i> |
|-------------|---------------------------------|------------------|---------------------|------------------------|
| | <i>Lat.(°N)</i> | <i>Lon.(°E)</i> | <i>Elevation(m)</i> | |
| Amdo (AD) | 32.24 | 91.62 | 4695 | alpine steppe |
| Ali (AL) | 32.49 | 80.10 | 4350 | bare soil |
| Bange (BG) | 31.40 | 90.14 | 4700 | alpine steppe |

| | | | | |
|-----------|-------|--------|------|---------------|
| Biru (BR) | 31.48 | 93.68 | 4408 | alpine steppe |
| US-AR1 | 36.42 | -99.42 | 611 | grassland |
| AT-Neu | 47.12 | 11.32 | 970 | grassland |

108 **3. Results**

109 **3.1 The impact of snow on the surface albedo at the TP sites**

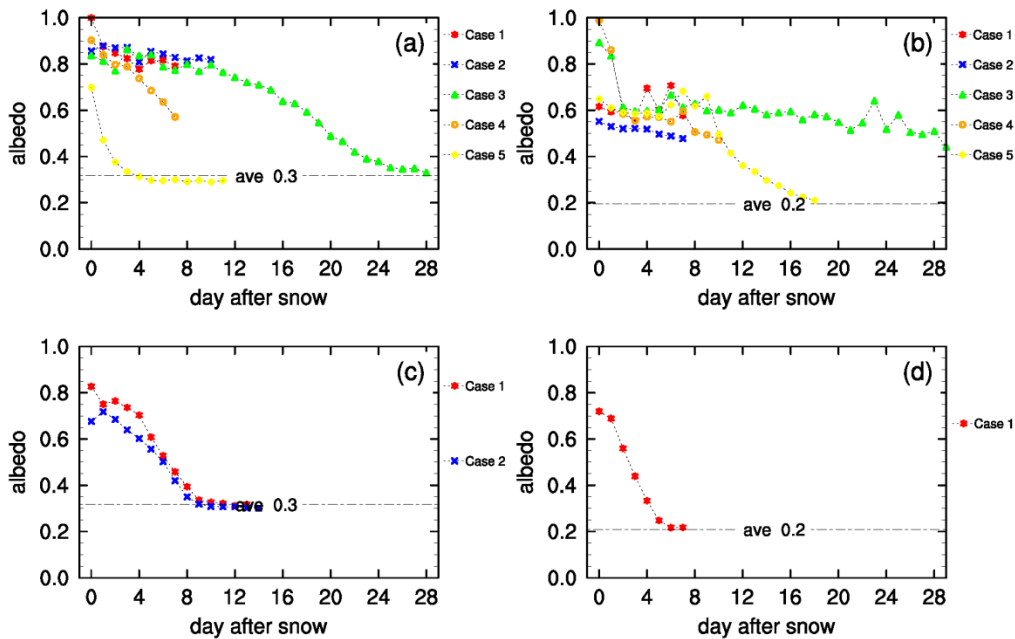
110 To investigate the impact of snow events on the surface energy balance over the TP,
111 we gathered 13 snow cases during the period from winter 2014 to spring 2016 from
112 the four observation sites in the TP (Table 2). Although there are snow water
113 equivalent (SWE) data measured by rain gauges at these sites, the data may be
114 severely underestimated. The underestimation is mainly due to the trajectory of the
115 falling snowflakes disturbed by strong winds and to the evaporation induced by
116 heating devices (Sevruk et al., 1989; Rasmussen et al., 2012; Grossi et al., 2017). In
117 particular, both the heating and wind speed are high over the TP. As an alternative, we
118 used land surface albedo to judge whether snow cover exists or not, since the land
119 surface albedo can be changed by snow cover (Warren 1982; Cline 1997). All 13
120 cases at the four TP sites capture the response of the land surface albedo to snow
121 processes (Figure 2) lthough the accumulation of the snow-water equivalent (SWE)
122 and snow cover duration are different from each other. Before snowfall, the monthly
123 mean albedo at Amdo (AD), Biru (BR), Bange (BG), and Ali (AL) are 0.3, 0.2, 0.3,
124 and 0.2, respectively. After a snowfall, the albedo clearly increases. The albedo on the
125 first day after snow is almost 0.99 and then decreases daily (e.g., Case #1 and Case #4
126 at the AD site and Case #4 at the BR site). The time series of the albedo generally
127 show gradual decreases for almost all snow cases, although with different rates of

128 decrease.

129 **Table 2.** Snow cases from the four observation sites in the TP, in which snow cover duration
 130 means the time from the beginning of snowfall to the time when the snow is melted

| | <i>Site</i> | <i>Snow cover duration</i> |
|----|-------------|-------------------------------|
| AD | Case1 | Dec. 15, 2014 – Dec. 23, 2014 |
| | Case2 | Dec. 24, 2014 – Jan. 3, 2015 |
| | Case3 | Jan. 4, 2015 – Feb. 3, 2015 |
| | Case4 | Jan. 20, 2016 – Jan. 27, 2016 |
| | Case5 | Jan. 30, 2016 – Feb. 15, 2016 |
| BR | Case1 | Dec. 18, 2014 – Dec. 25, 2014 |
| | Case2 | Dec. 26, 2014 – Jan. 2, 2015 |
| | Case3 | Jan. 7, 2015 – Feb. 6, 2015 |
| | Case4 | Jan. 7, 2016 – Jan. 20, 2016 |
| | Case5 | Jan. 21, 2016 – Feb. 8, 2016 |
| BG | Case1 | Dec. 17, 2014 – Dec. 30, 2014 |
| | Case2 | Jan. 6, 2015 – Jan. 20, 2015 |
| AL | Case1 | Mar. 3, 2015 – Mar. 8, 2015 |

131



132

133 **Figure 2** Evolution of the albedo after snow for the snow cases at the four TP sites: (a) AD; (b)

134 BR; (c) BG; (d) AL. The dash-dotted line is the monthly mean albedo before snow.

135 **3.2 Quantitative analysis of the impact of snow on the turbulent fluxes at the TP**
136 **sites**

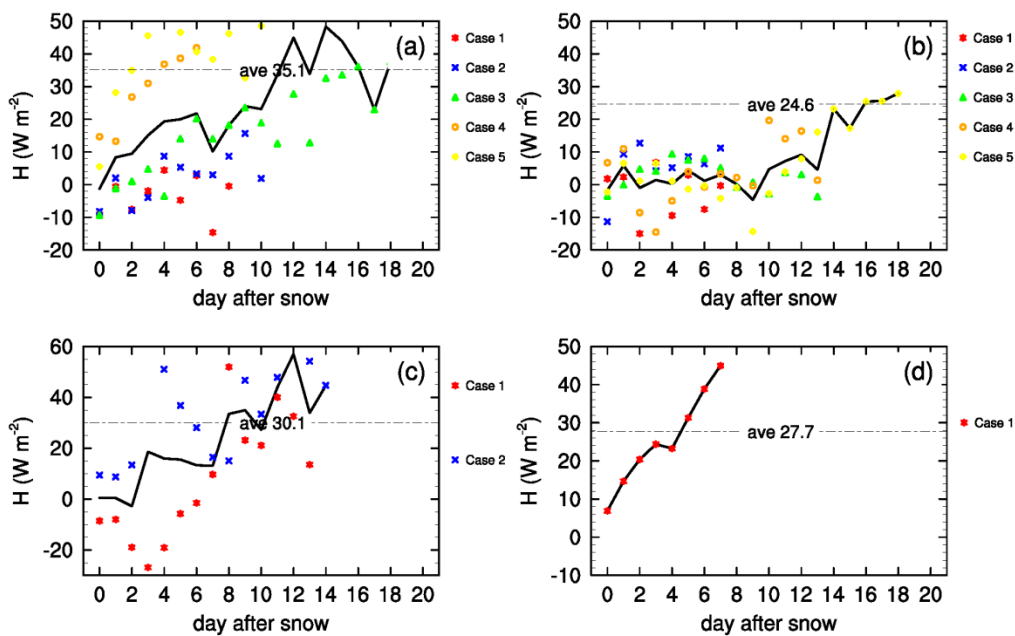
137 The effect of snow on H is presented in Table 3 and Figure 3. The daily maximum
138 Hs before (after) snow are 239.5 (137.3), 164.1 (77.4), 167.2 (96.1), 158.1 (124.0) W
139 m⁻² at the AD, BR, BG, and AL sites, respectively (Table 3). Furthermore, the
140 standard deviation (σ) of H after snow is smaller than that before snow (Table 3). The
141 above results clearly indicate that the value and varying magnitude of H after snow is
142 smaller than that before snow for the TP sites. Clearly, the snow reduces the transfer
143 of H from the land surface to the atmosphere.

144 **Table 3** The daily maximum value and standard deviation (σ) of H (W m⁻²) and LE (W m⁻²)
145 before (monthly mean value) and after (case-averaged value) snow for the four TP sites

| Site | H | | | | LE | | | |
|------|--------------------------------|-------|-------------------------------|-------|--------------------------------|-------|-------------------------------|-------|
| | Daily max (W m ⁻²) | | σ (W m ⁻²) | | Daily max (W m ⁻²) | | σ (W m ⁻²) | |
| | Before | After | Before | After | Before | After | Before | After |
| AD | 239.5 | 137.3 | 87.0 | 49.0 | 29.8 | 98.5 | 9.3 | 30.9 |
| BR | 164.1 | 77.4 | 53.9 | 27.6 | 30.5 | 68.1 | 8.6 | 20.0 |
| BG | 167.2 | 96.1 | 59.8 | 41.8 | 25.0 | 34.4 | 7.3 | 10.4 |
| AL | 158.1 | 124.0 | 51.9 | 35.7 | 24.3 | 73.6 | 6.9 | 18.9 |

146 Figure 3 further presents the daily evolution of H during the snow cover duration.
147 On the first day after snow, sharp decreases in H occur, with the case-averaged Hs
148 decreasing to -1.0, -1.7, 0.4, and 6.9 W m⁻² at the AD, BR, BG, and AL sites,
149 respectively. These Hs are much lower than those (approximately 35.1, 24.6, 30.1, and
150 27.7 W m⁻², respectively) before snow at the four sites. During the following days, the
151 Hs gradually recover (Figure 3). The mean H of all cases at the four TP sites (Figure

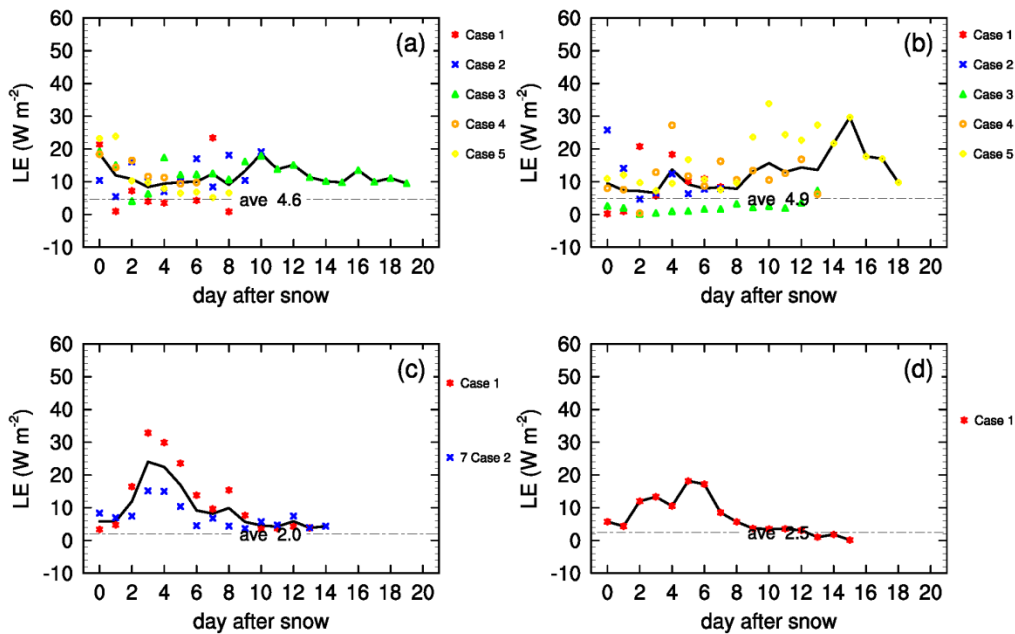
152 5a) further confirms the begining decrease and the following slow recovery of the H.
 153 This process of evolution of H maintains for almost two weeks. The recovery process
 154 of H mainly depends on the terrain and weather conditions (e.g., the amount of snow,
 155 air temperature, solar radiation, and wind speed). For the AD, BR, BG, and AL sites,
 156 the case-average recovery periods of H are approximately 11, 15, 10, and 5 days,
 157 respectively. The average recovery period of all 13 cases is approximately 13 days
 158 (Figure 5a).



159
 160 **Figure 3.** Time series of the daily mean H (units: $W m^{-2}$) after snowfall for the snow cases at the
 161 four TP sites: (a) AD; (b) BR; (c) BG; (d) AL. The dash-dotted line is the monthly mean value
 162 before snow, and the solid line is the case-average value.

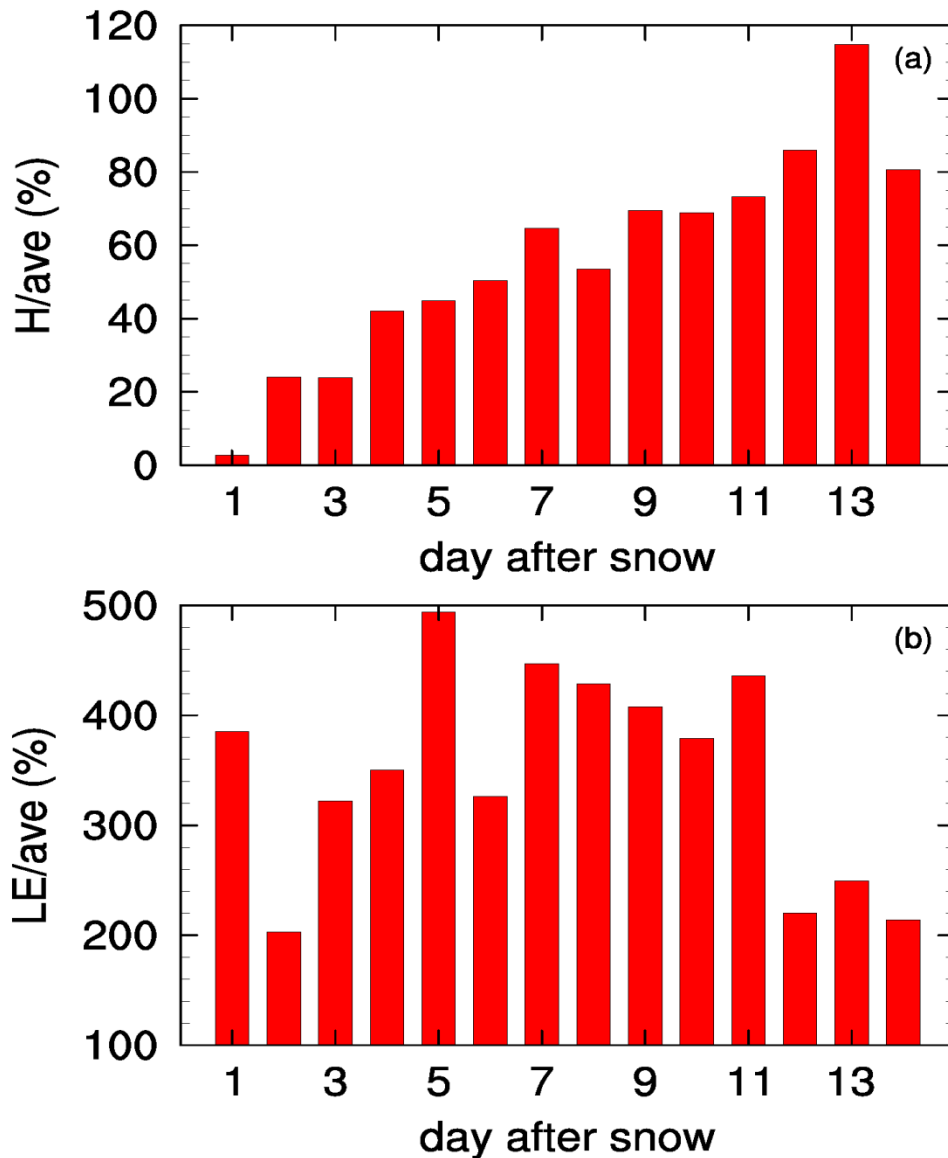
163 Different from H, the daily maximum and mean values and standard deviation (σ)
 164 of LE are smaller before snow than after snow (Table 3 and Figure 4). This signifies
 165 that the LE becomes stronger and more active after snowfall, suggesting that the snow
 166 enhances the transfer of LE from the land surface to the atmosphere.

167 The peak of the LE increased by snow is not on the first day but in the next few
 168 days (Figures 4 and 5). The reason is probably that the time when the LE reaches the
 169 peak mainly depends on the time of the maximum snowmelt. When the LE reaches
 170 the peak, its value is approximately 500% of that before snow (Figure 5). Additionally,
 171 the evolution process of LE persists for a longer period than the recovery period of H,
 172 since the soil moisture content may still contribute to a high LE after the
 173 disappearance of snow cover (Figure 4).



174

175 **Figure 4.** As in Figure 3, but for the LE



176

177 **Figure 5** The histograms of the ratio of daily mean H (a) and LE (b) after snow to the average

178 value before snow

179 **3.3 Impact on the TP surface heating**

180 As indicated above, snow reduces H but increases LE, and meanwhile results in

181 different evolution processes of H and LE. Several studies have documented the

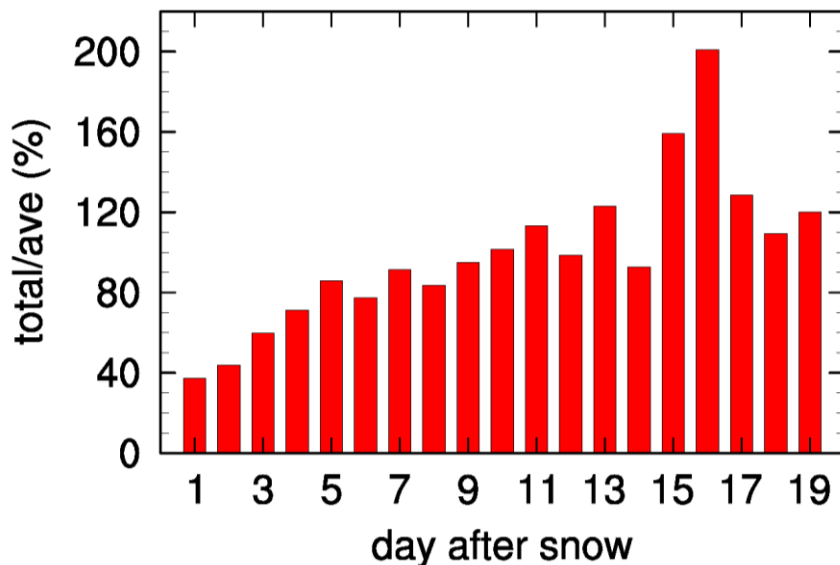
182 importance of land surface heating in modulating weather and climate changes over

183 the TP (Wu et al., 1998; Hsu and Li, 2003; Rajagopalan et al., 2013; Wang et al.,

184 2019). Certainly, it is also important to further explore the total effect of snow on the

185 surface turbulent flux (i.e., the sum of H and LE), which is regarded as a crucial
186 component of the heat source of the TP.

187 On the first day after snow, the surface turbulent flux rapidly decreases to
188 approximately 39% of that before snow (Figure 6), from 36.7 W m^{-2} to 13.6 W m^{-2} .
189 This causes a weaker surface heating of the TP. This heating maintains a weaker level
190 than before snow for approximately 10 days, although gradually increasing, and then
191 recovers to the magnitude before snow after 10 days. As shown in Section 3.2, the H
192 recovers to the original level after the snowmelt, but the LE still maintains and even
193 increases to a higher level because of the soil moisture anomalies caused by the
194 snowmelt. Thus, the joint effect of H and LE seems to result in the even larger heating
195 of the TP after the snowmelt than before snow; that is, the stronger heating tends to
196 appear after the process of snowfall (Figure 6). The remarkable fluctuation of the
197 surface heating of the TP associated with snow events may exert a pronounced
198 influence on local and downstream weather processes.

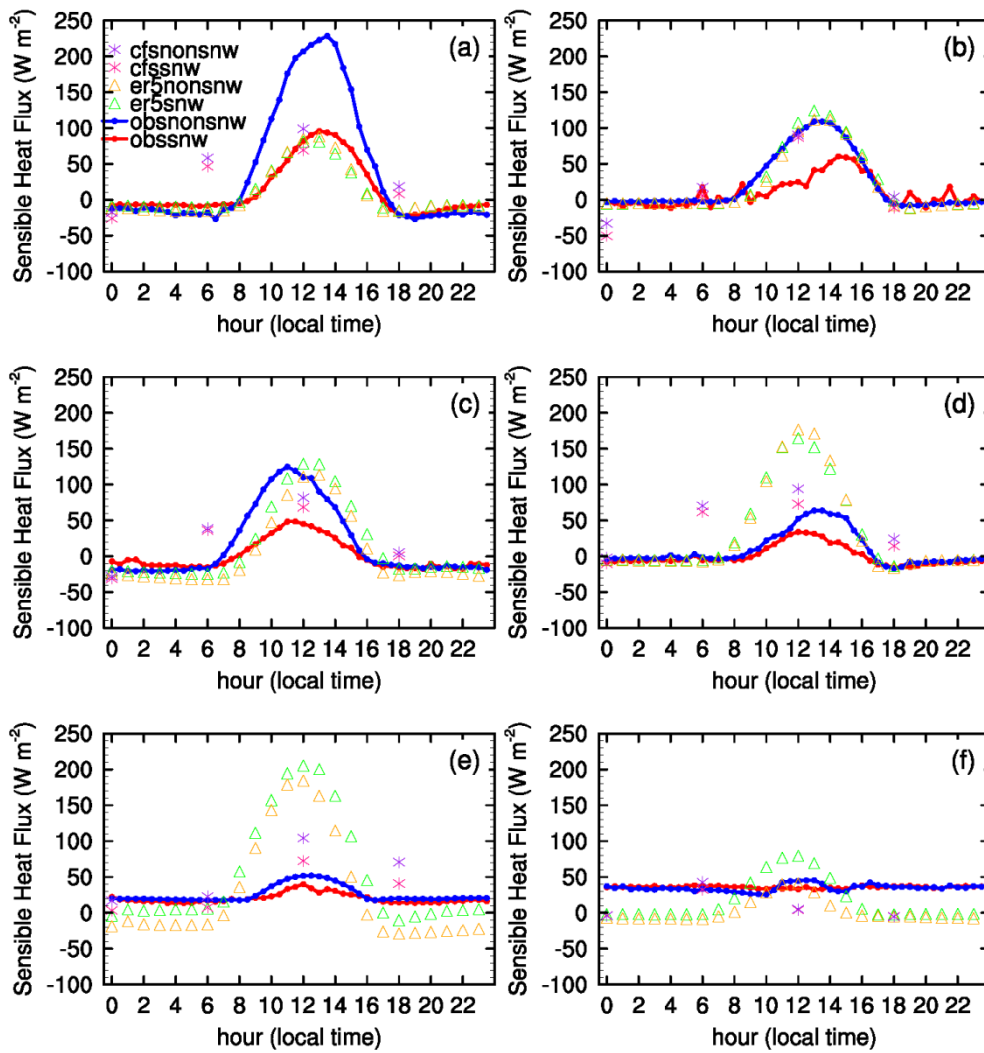


200 **Figure 6** The histogram of the ratio of the daily mean of the turbulent heat flux (i.e., the sum of H
201 and LE) after snow to the average turbulent heat flux before snow

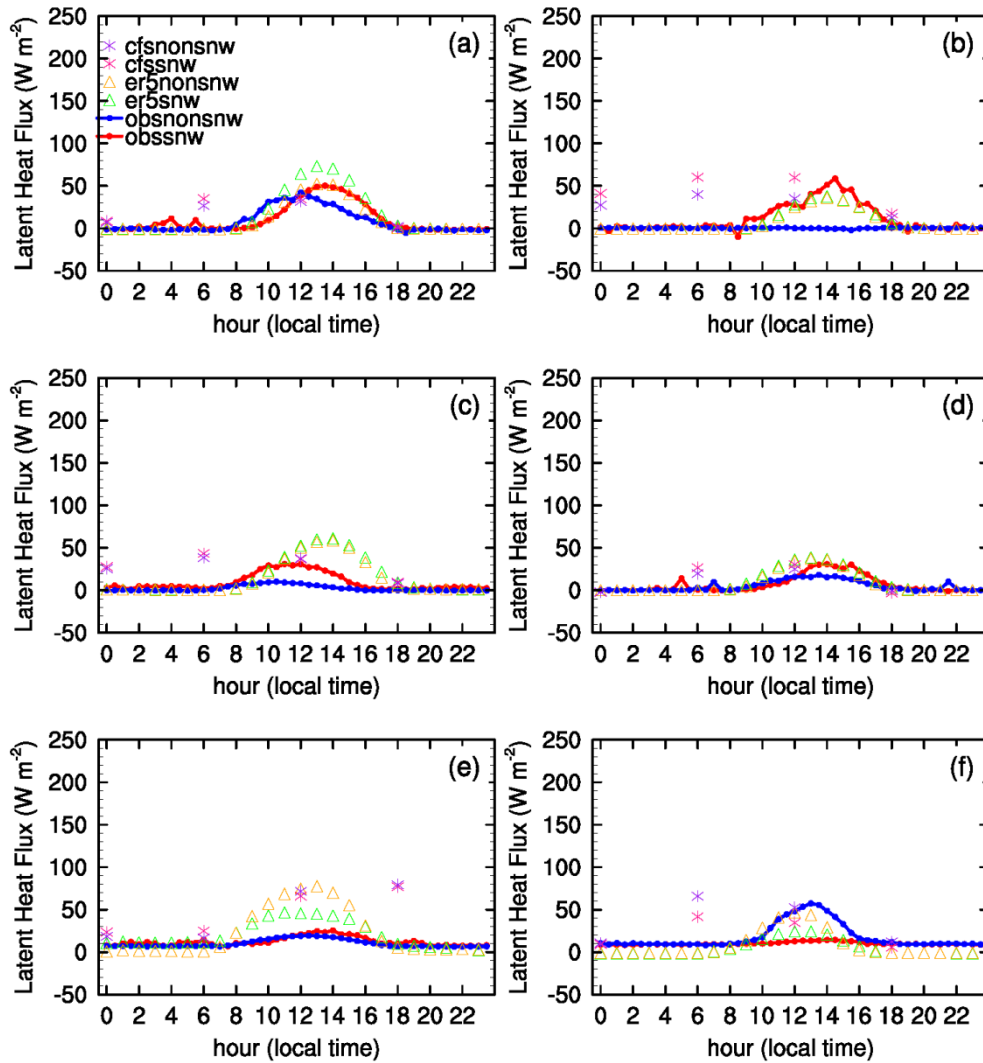
202 **3.4 Comparison between the surface heat fluxes over the TP and over the** 203 **low-altitude regions.**

204 The surface heat fluxes (H and LE) over the TP are considerably affected by snow,
205 as shown in the previous subsections. We wonder whether the impact of snow is
206 different between the TP and low-altitude regions. To more clearly and detailly
207 demonstrate the differences of the surface heat fluxes affected by snow between
208 different regions, the multi-winter-averaged diurnal cycles for the four sites in the TP
209 and the two sites in the low regions are presented in Figures 7 and 8. As shown in
210 Figure 7a-d, the H with snow cover (red line) is much lower than that without snow
211 cover (blue line) at the four TP sites. The maximum value (59.7 W m^{-2}) of the
212 site-averaged H during the snow cover period, which generally appears at noon and
213 afternoon, is much lower than that (131.5 W m^{-2}) during the non-snow cover period. In
214 contrast, at the two low-altitude sites, the difference between the H with snow cover
215 and that without snow cover is very small (Figure 7e, f). The maximum value (35.5 W
216 m^{-2}) of the site-averaged H during the snow cover period does not show a large
217 decrease relative to that (46.7 W m^{-2}) during the non-snow cover period. The results
218 revealed that H is largely decreased by snow cover over the TP, whereas the effect of
219 snow cover in reducing the H is much weaker over the low-altitude regions. The mean
220 absolute difference (MAD) further shows that at noon and afternoon of local time, the
221 differences between the H with snow cover and that without snow cover at the four

222 TP sites (see black curves in Figures 10a–d) are clearly larger than those at the two
 223 low-altitude sites (see black curves in Figures 10e–f). Similarly, the LE is remarkably
 224 increased by snow cover over the TP, and the effect of snow cover on the LE is also
 225 weaker over the low-altitude regions (Figure 8; the figure of MADs in LE is not
 226 shown).



227
 228 **Figure 7** Multiwinter-averaged diurnal cycle of H for snow cover and non-snow cover conditions
 229 at (a) Amdo, (b) Ali, (c) Bange, (d) Biru, (e) US-AR1, and (f) AT-Neu. “cfs” means CFS; “er5”
 230 means ERA5; “obs” means observation; “nonsnw” means non-snow cover; “snw” means snow
 231 cover



232

233 **Figure 8** As in Figure 7, but for the LE

234 The difference in the surface heat flux between the snow cover and non-snow
 235 cover conditions is larger at noon and afternoon. This implies that the solar radiation
 236 may be responsible for, at least partly, such a difference. Relative to that at the
 237 low-altitude sites, the surface net solar radiation (R_n) at the TP sites shows larger
 238 differences between the snow cover and non-snow cover conditions (Figure 9). The
 239 daily maximum R_n with (without) snow cover is 102.2 W m^{-2} (369.7 W m^{-2}) at the TP
 240 sites, whereas that with (without) snow cover is 58.5 W m^{-2} (134.0 W m^{-2}) at the
 241 low-altitude sites. The results imply that the stronger modulation of the H and LE by

242 snow over the TP may be partly attributed to the larger and more drastic change of the
243 R_n associated with snow processes in this high-altitude region.

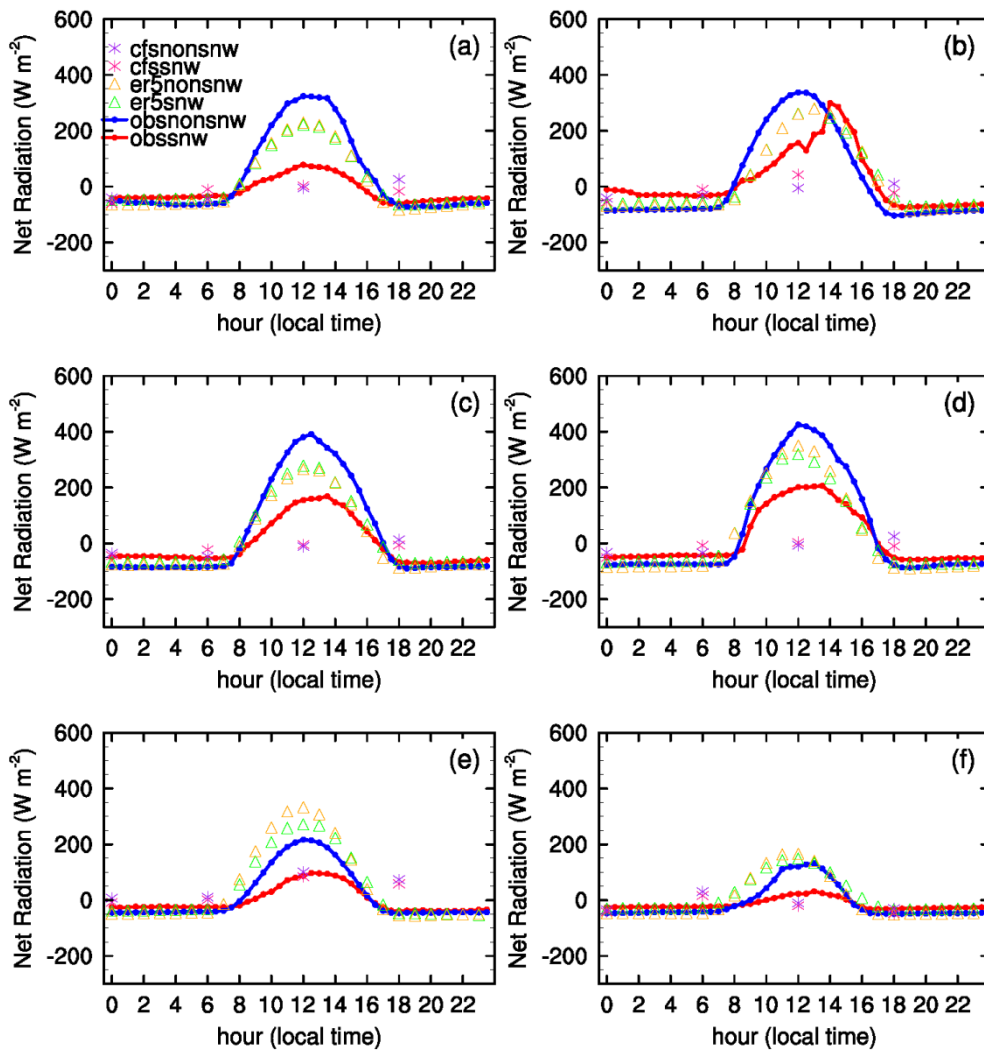
244 By calculating bias error (BE) and mean absolute error (MAE), we further
245 compared the ERA5 and CFS reanalysis datasets (Table 4). The results show that
246 relative to the CFS, the ERA5 has smaller MAEs for H, LE, and R_n at the TP sites, but
247 larger MAEs for H at the low-altitude sites (Table 4). Generally speaking, the heat
248 fluxes of the ERA5 reanalysis seem more reliable than those of the CFS reanalysis.
249 However, the ERA5 reanalysis severely underestimates the difference between the H
250 with snow cover and that without snow cover (red stars in Figures 10a–d), although it
251 shows a higher reliability of the heat fluxes than the CFS reanalysis over the TP.
252 Different from the results over the TP, the ERA5 reanalysis overestimates the
253 difference between the H with snow cover and that without snow cover at the
254 low-altitude sites (red stars in Figures 10e–f). The CFS reanalysis is worse, since it
255 even cannot capture the basic diurnal cycle of the fluxes (Figures 7 and 8) and
256 certainly cannot reproduce the observational difference between the H with snow
257 cover that without snow cover (triangles in Figure 10). In summary, both the ERA5
258 and CFS reanalysis datasets fail to reproduce the modulation of snow on the heat
259 fluxes. Therefore, the physical schemes of the models, particularly the snow scheme,
260 should be further improved based on the observational analysis over TP.

261 **Table 4** Bias error (BE, $W m^{-2}$) and mean absolute error (MAE, $W m^{-2}$) of H, LE and R_n
262 between the reanalyses (ERA5 and CFS) and observation at the six sites

| site | ERA5 | CFS |
|------|------|-----|
|------|------|-----|

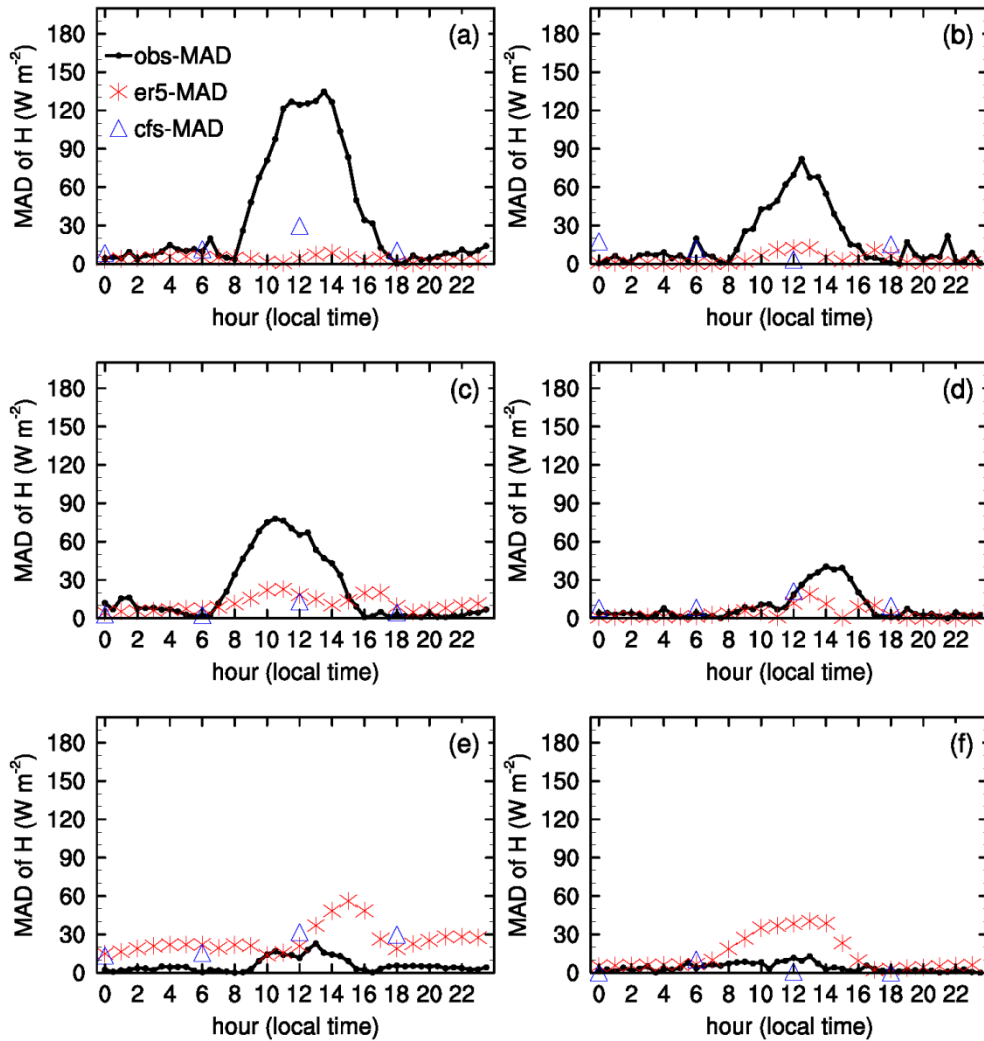
| | H | | LE | | R _n | | H | | LE | | R _n | |
|----|-------|------|------|------|----------------|------|-------|------|------|------|----------------|-------|
| | BE | MAE | BE | MAE | BE | MAE | BE | MAE | BE | MAE | BE | MAE |
| AD | -10.4 | 16.3 | 4.5 | 6.5 | 18.1 | 39.3 | 9.8 | 36.6 | 9.0 | 12.8 | -18.2 | 60.9 |
| AL | -1.6 | 5.3 | 6.7 | 7.8 | 0.1 | 39.4 | -1.0 | 17.1 | 28.9 | 28.9 | -33.2 | 132.2 |
| BG | 2.1 | 22.3 | 9.3 | 11.9 | 1.7 | 36.2 | 13.2 | 28.5 | 22.5 | 22.4 | -32.8 | 101.6 |
| BR | 31.1 | 31.9 | 3.0 | 4.7 | 6.7 | 37.6 | 34.6 | 35.8 | 6.9 | 11.7 | -37.1 | 87.8 |
| US | 3.2 | 47.9 | 16.5 | 20.0 | 33.6 | 42.3 | 26.5 | 27.8 | 33.6 | 36.4 | 28.4 | 74.1 |
| AT | -25.3 | 33.0 | -7.0 | 9.5 | 22.1 | 25.4 | -28.5 | 30.8 | 13.9 | 14.9 | -8.0 | 43.1 |

263



264

265 **Figure 9** As in Figure 7, but for the R_n



266

267 **Figure 10** Diurnal cycle of the mean absolute difference (MAD, W m^{-2}) of H between snow and

268 no snow for observation, ERA5 and CFS at (a) Amdo, (b) Ali, (c) Bange, (d) Biru, (e) US-AR1,

269 and (f) AT-Neu. “obs”, “cfs”, and “er5” denote observation, CFS, and ERA5.

270 **4. Conclusions and Discussion**

271 Through modulating surface heating, the snow cover over the TP has an

272 influence on the Asian atmospheric circulation and weather during winter (Li et al.,

273 2018). However, a key issue—how and by how much is the surface heating of the TP

274 modulated by snow? —remains unclear, in particular, the daily evolution of surface

275 heating of the TP adjusted by snow has not been revealed because of the lack of
276 observational data. Using the eddy-covariance, atmospheric gradient, and solar
277 radiation measurements from the 4 sites in the TP obtained from the TIPEX-III, the
278 snowfall-related daily evolution of the surface turbulent heating (i.e, H and LE) is
279 investigated. The results show that the surface albedo sharply increases to almost 1 on
280 the first day of snow and then gradually decreases. Correspondingly, the H flux
281 sharply decreases after snow, with a smaller value and varying magnitude than that
282 before snow. That is, the snow can suppress the transfer of H from the land surface to
283 the atmosphere. During the following approximately 10 days after snow, H gradually
284 recovers to the original level. In contrast to H, the LE becomes stronger and more
285 active after snowfall, indicating that the snow can enhance the transfer of LE from the
286 land surface to the atmosphere. The fluctuation of LE resulted from snow can persist
287 for a longer period than H, since the soil moisture may still contribute to a high LE
288 after snowmelt. Although the effect of snow on the H and that on the LE are opposite
289 to each other, the joint effect on the total turbulent flux (i.e, the sum of H and LE) is
290 clear: the surface turbulent heating of the TP decreases at the early period of snow
291 events and then even enhances to a higher level after the snowmelt than before snow.
292 The severe fluctuation resulted from snowfall may affect local and downstream
293 atmospheric circulation and weather processes during winter, which deserves further
294 study in the future.

295 Comparison analyses preliminarily reveal that the impact of snow on the H and
296 LE over the TP is much stronger than over similar latitude low-altitude regions in

297 North America and Europe. This difference may be partly attributable to the larger
298 and more drastic change of the surface net solar radiation associated with snow
299 processes in the TP. However, the detailed processes should be explored in future
300 research. For example, the solar radiation-snowmelt surface heating link and
301 evolution processes in different latitude regions require further investigation.

302 The ERA5 and CFS reanalysis datasets fail to reproduce the effect of snow on the
303 surface heat fluxes over the TP and low-altitude regions. This indicates caution should
304 be taken when using the reanalysis surface heat fluxes to diagnose the TP
305 heating-related synoptic processes. After obtaining more flux observations in the TP,
306 we will continue to verify the daily fluctuation of the surface heating of the TP
307 associated with snow events. This is conducive to understand the detailed physical
308 processes of modulation of snow events on Asian weather processes during winter and
309 the improvement of surface parameterization schemes of the surface energy balance
310 in the land surface models.

311 **Acknowledgments:**

312 This research was funded by the National Key Research and Development Program of
313 China (Grant 2018YFC1505706), the Strategic Priority Research Program of the
314 Chinese Academy of Sciences (Grant XDA20100300), the Second Tibetan Plateau
315 Scientific Expedition and Research (STEP) program (2019QZKK0105), the Science
316 and Technology Development Fund of CAMS (Grant 2019KJ022) and the Basic
317 Research Fund of CAMS (Grant 2019Z008).

318 **Data Availability Statement**

319 The in-situ data of six sites can be found at
320 <https://doi.org/10.6084/m9.figshare.14471283>; The ERA5 reanalysis dataset were
321 publicly provided by European Centre for Medium-Range Weather Forecasts
322 ([https://cds.climate.copernicus.eu/cdsapp#!/dataset/10.24381/cds.e2161bac?tab=overv](https://cds.climate.copernicus.eu/cdsapp#!/dataset/10.24381/cds.e2161bac?tab=overview)
323 [iew](https://cds.climate.copernicus.eu/cdsapp#!/dataset/10.24381/cds.e2161bac), DOI:10.24381/cds.e2161bac); The CFS reanalysis datasets were publicly
324 provided by National Oceanic and Atmospheric Administration
325 (<https://rda.ucar.edu/datasets/ds094.1/>, DOI: 10.5065/D6N877VB).

326 **References**

327 Bolin, B., 1950: On the influence of the earth's orography on the westerliers. *Tellus*, 2,
328 184-195.

329 Charney, J. G., and A. Eliassen, 1949: A numerical method for predicting in the
330 perturbation of the middle latitude westerlier. *Tellus*, 1, 38-54

331 Chen, J., and S. Bordoni., 2013: Orographic effects of the Tibetan Plateau on the East
332 Asian Summer Monsoon: An Energetic Perspective. *J. Climate*, 27, 3052-3072

333 Chen, F., Barlage, M., Tewari, M., et al., 2014: Modeling seasonal snowpack
334 evolution in the complex terrain and forested colorado headwaters region: a
335 model inter-comparison study. *J. Geophys Res. Atmos.*, 119(24), 13,795-113,819.

336 Chen, J. M., X. Yue, G. Liu, S. Nan. 2020. Relationship between the thermal
337 condition of the Tibetan Plateau and precipitation over the region from eastern
338 Ukraine to north Caucasus during summer. *Theoretical and Applied Climatology*,
339 142, 1379–1395.

340 Chen G. S., Liu Z., and Kutzbach J. E.,2014: Reexamining the barrier effect of the
341 TibetanPlateau on the South Asian summer monsoon.*Clim. Past*, 10: 1269–75.

342 Chen, Q. J., B. Gao., and W.J. Wei, 2000: Studies on relationshipsamong winter snow
343 cover over the Tibetan Plateau and droughts/floods during Meiyu season in the
344 middle and lower reaches ofthe Changjiang river as well as in the
345 atmosphere/ocean system(in Chinese). *Acta Meteorol. Sin.*, 58, 582–595.

346 Cline, D. W., 1997: Snow surface energy exchanges and snowmelt at a continental,
347 midlatitude Alpine site. *Water resources research*, 33, 689-701

348 Dey, B., and O. S. R. U. Bhanukumar,1983: Himalayan winter snow cover area and
349 summermonsoon rainfall over India. *J. Geophys. Res.*, 88, 5471–5474.

350 Dey, B.,S. N. Kathuria, and O. B. Kumar, 1985: Himalayan summersnow cover and
351 withdrawal of the Indian summer monsoon. *J.Appl. Meteor.*, 24, 865–868.

352 Dey, B.,and S. N. Kathuria, 1986: Himalayan snow cover area andonset of summer
353 monsoon over Kerala, India. *Mausam*, 37, 193–196.

354 Duan A. M., G. X. Wu, 2005: Role of the Tibetan Plateau thermal forcing in the
355 summer climate patterns over subtropical Asia. *Climate Dyn.*, 24, 793-807.

356 Duan, A. M., Wang, M.-R., Lei, Y.-H., Cui, Y.-F., 2013. Trends in summer rainfall
357 over China associated with the Tibetan Plateau sensible heat source during 1980–
358 2008. *J. Clim.* 26(1), 261–275. <https://doi.org/10.1175/JCLI-D-11-00669.1>.

359 Flohn, H., 1957: Large-scale aspects of the “summer monsoon” in South and East
360 Asia. *J. Meteor. Soc. Japan*.35, 180-186.

361 Grossi, G., A. Lendvai,G. Peretti, et al., 2017: Snow precipitation measured by gauges:
362 Systematic error estimation and data series correction in the central Italian
363 Alps.*Water*, 9(7), 461, doi:10.3390/w9070461

364 He, H., J. W. McGinnis, Z. Song, and M. Yanai, 1987: Onset of the Asian summer
365 monsoon in 1979 and the effect of the Tibetan Plateau. *Mon. Wea. Rev.*, 115,
366 1966-1995.

367 Hsu, H. H., Xin L., 2003: Relationship between the Tibetan Plateau heating and East
368 Asian summer monsoon rainfall. *Geophys. Res. Letters*, 2003, 30(20):1182-1200.

369 Kanamitsu, M., W. Ebisuzaki, J. Woollen, et al., 2002: NCEP–DOE AMIP-II
370 reanalysis (R-2). *Bull. Amer. Meteor. Soc.*, 83, 1631–1643, doi:

371 10.1175/BAMS-83-11-1631.

372 Li, W., Guo, W. , Qiu, B. , Xue, Y. , Hsu, P. C., 2018: Influence of Tibetan Plateau
373 snow cover on East Asian atmospheric circulation at medium-range time scales.
374 *Nature Communications*,9(1).

375 Liu, G., R. Wu, Y. Zhang, 2014: The summer snow cover anomaly over the Tibetan
376 Plateau and its association with simultaneous precipitation over the Meiyu–Baiu
377 region. *Advances in Atmospheric Sciences*, 31 (4), 755-764.

378 Liu, G., Zhao P., Chen J.-M., 2017. Possible effect of the thermal condition of the
379 Tibetan Plateau on the interannual variability of the summer Asian-Pacific
380 Oscillation. *J. Clim.* 30, 9965–9977. <https://doi.org/10.1175/JCLI-D-17-0079.1>.

381 Liu, G., Zhao P., Chen J.-M., Yang S., 2015. Preceding factors of summer Asian–
382 Pacific oscillation and the physical mechanism for their potential influences. *J.*
383 *Clim.* 28, 2531–2543. <https://doi.org/10.1175/JCLI-D-14-00327.1>.

384 Liu X., G. X. Wu, W. P. Li et al., 2001: Thermal adaptation of the large-scale
385 circulation to the summer heating over the Tibetan Plateau (in Chinese), *Porg.*
386 *Nat. Sci.*, 11, 207-214

387 Liu X., W. P. Li, and G. X. Wu, 2002: Interannual variations of the diabatic heating
388 over the Tibetan Plateau and the northern hemispheric circulation in summer.
389 *Acta Meteor. Sin.*, 60, 267-277.

390 Liu Y. M, Wu GX and Hong JL *et al.* 2012:Revisiting Asian monsoon formation
391 andchange associated with Tibetan Plateau forcing: II. change. *Clim.Dyn.*,39:
392 1183 – 9

393 Lu, M.-M, Yang, S., Li, Z.-N., He, B., He, S., Wang, Z.-Q., 2018. Possible effect of
394 the Tibetan Plateau on the "upstream" climate over West Asia, North Africa,
395 South Europe and the North Atlantic. *Clim. Dyn.* 51(4), 1485–1498.

396 Luo, H., and M. Yanai, 1983: The large-scale circulation and heat sources over the
397 Tibetan Plateau and surrounding areas during the early summer of 1979. Part I:
398 Precipitation and kinematic analysis, *Mon. Wea. Rev.*, 111, 922-944

399 Luo, H., and M., Yanai, 1984: The large-scale circulation and heat sources over the
400 Tibetan Plateau and surrounding areas during the early summer of 1979. Part II:
401 heat and moisture budgets, *Mon. Wea. Rev.* 112, 966-989

402 Ma, D., Boos W. and Kuang Z. M. 2014: Effects of orography and surface heat
403 fluxeson the South Asian summer monsoon. *J.Clim.*27: 6647 – 59.

404 Muñoz Sabater, J., 2019: ERA5-Land hourly data from 1981 to present. Copernicus
405 Climate Change Service (C3S) Climate Data Store (CDS). [http:// DOI:](http://DOI:10.24381/cds.e2161bac)
406 10.24381/cds.e2161bac

407 Nan, S., P. Zhao, 2012: Snowfall over central-eastern China and Asian atmospheric
408 cold source in January. *Int. J.Climatol.*, 32:888-899.

409 Nan, S. L., Zhao, P., Chen, J. M., 2019. Variability of summertime Tibetan
410 tropospheric temperature and associated precipitation anomalies over the
411 central-eastern Sahel. *Clim. Dyn.* 52(3–4), 1819–1835

412 Nan, S., L., P. Zhao, J. Chen, G. Liu. Links between the thermal condition of the
413 Tibetan Plateau in summer and atmospheric circulation and climate anomalies
414 over the Eurasian continent. *Atmos. Res.*, 247, 10.1016/j.atmosres.2020.105212

415 Nitta, T., 1983: Observational study of heat sources over the eastern Tibetan Plateau
416 during the summer monsoon. *J. Meteor. Soc. Japan*, 61, 590-605

417 Queney, P., 1948: The problem of air flow over mountains :A summary of theoretical
418 studies. *Bull. Amer. Meteor. Soc.*, 29, 16-29.

419 Rajagopalan, B., et al., 2013: Signatures of Tibetan Plateau heating on Indian summer
420 monsoon rainfall variability. *J. Geophys. Res. Atmos.*, 118(3), 1170-1178.

421 Rasmussen, R. B. Baker, J. Kochendorfer, et al., 2012: How well are we measuring
422 snow? The NOAA/FAA/NCAR winter precipitation test bed. *Bull. Amer. Meteor.*
423 *Soc.* 6, 811–829.

424 Sevruk, B. 1972: Distribution of precipitation in mountainous areas. In *Evaporation*
425 *Losses from Storage Gauges*; WMO: Geneva, Switzerland, pp. 96–102.

426 Sevruk, B., J. Hertig, R. Spiess, 1989: Wind field deformation above precipitation
427 gauge orifices. *IAHS*, 179, 65–70.

428 Shen, Z., D. Weng, and S. Pan, 1984: An outline of the Qinghai-Xizang Plateau heat
429 source observation experiment. *Collected Papers on the Qinghai-Xizang Plateau*
430 *Meteorological Experiment* (in Chinese), Science Press, 1-9

431 Tao S. Y., and L. Chen, 1987: A review of recent research on the East Asian summer
432 monsoon in China. *Monsoon Meteorology*, C. P. Zhang and T. N. Krishnamurti
433 Eds., Oxford University Press, 60-92.

434 Warren, S. G. ,1982: Optical properties of snow. *Reviews of Geophysics*, 20.

435 Wei, Z. G., and S.W. Luo, 1994: Influence of snow cover in westernChina on
436 precipitation in the flood period in China (in Chinese).*Plateau Meteor.*, 14, 347–
437 354.

438 Wu, T. W., and Z. A. Qian, 2000: Further analyses of the linkagebetween winter and
439 spring snow depth anomaly over Qinghai-Xizang Plateau and summer rainfall of
440 eastern China (in Chinese).*Acta Meteorol. Sin.*, 58, 570–581.

441 Wu, T. W., et al., 2003: The relation between the Tibetan winter snow and the Asian
442 summer monsoon and rainfall: An observational investigation. *J. Climate*, 16(12),
443 2038-2051.

444 Wu G. X., and Coauthors, 1997: The LASG global ocean-atmosphere-land system
445 model GOALS/LASG and its simulation study. *Appl. Meteor.*, 8, 15-28.Wu, G,
446 Zhang Y., 1998: Tibetan Plateau Forcing and the Timing of the Monsoon Onset
447 over South Asia and the South China Sea. *Mon. Wea. Review*, 126(126):913-927.

448 Wu, G. X., and Y. Liu, 2003: Summertime quardruplet heating pattern in the
449 subtropics and the associated atmospheric circulation. *Geophys. Res. Lett.*, 30,
450 1201.

451 Wu, G. X., 2004: Recent progress in the study of the Qinghai-Xizang Plateau climate
452 dynamics in China. *Quart. Sci.*, 24, 1-9.

453 Wu, G. X., Zhou, H. F., Wang, Z.-Q., Liu, Y. M., 2016. Two types of summertime
454 heating over Asian large-scale orography and excitation of potential-vorticity
455 forcing I. over Tibetan Plateau. *Sci. China Earth Sci.* 59, 1996–2008.

456 Xu, G. C., S. Li, and B. Hong, 1994: The influence of the abnormal snow cover over
457 the Qinghai-Tibet Plateau on Chinese precipitationand atmospheric circulation
458 (in Chinese). *Quart. J. Appl. Meteor.*, 5, 62–67.

459 Xin, Y. F., F. Chen., P. Zhao. et al., 2018: Surface energy balance closure at ten sites
460 over the Tibetan Plateau. *Agricultural and Forest Meteorology*, 259, 317-328.

461 Yanai, M., C. F. Li and Z. S. Song, 1992: Seasonal heating of the Tibetan Plateau and
462 its effects on the evolution of the Asian Summer Monsoon. *J. Meteor. Soc.*
463 *Japan*, 70, 319-351

464 Yanai, M., and C. Li, 1994: Mechanism of heating and the boundary layer over the
465 Tibetan Plateau. *Mon. Wea. Rev.*, 122, 305-323.

466 Yanai and G. X. Wu, 2006: Effect of the Tibetan Plateau. *The Asian Monsoon*. B.
467 Wang, Ed., Springer, 513-549

468 Yeh, T. C., 1950: The circulation of high troposphere over China in winter of 1945-46.
469 *Tellus*, 2, 173-183.

470 Yeh, T. C., Lo, S. W., Chu, P. C. 1957: The wind structure and heat balance in the
471 lower troposphere over Tibetan Plateau and its surrounding. *Acta. Meteorol. Sin.*
472 28: 108-21

473 Yeh T. C. and Y. X. Gao 1979: *Meteorology of Qinghai-Xizang Plateau*. Chinese
474 Science Press, 278pp

475 Yin, M., 1949: A synoptic-aerological study of the onset of the summer monsoon over
476 India and Burma. *J. Meteor.*, 6: 393-400

477 Zhai, P. M., and Q.-F. Zhou, 1997: The change of Northern Hemisphere snow cover
478 and its impact on summer rainfall in China (in Chinese). *Quart. J. Appl. Meteor.*,
479 8, 231-235.

480 Zhao, P., Z. J. Zhou, and J. P. Liu, 2007: Variability of Tibetan spring snow and its
481 associations with the hemispheric extratropical circulation and East Asian
482 summer monsoon rainfall: An observational investigation. *J. Climate*, 20, 3942-
483 3955,

484 Zhao, P., X. Xu, F., Chen et al., 2018: The Third Atmospheric Scientific Experiment
485 for Understanding the Earth-Atmosphere Coupled System over the Tibetan
486 Plateau and Its Effects. *Bull. Amer. Meteor. Soc.* 99(4), 757-776

487